JOURNAL OF OPTOELECTRONICS AND ADVANCED MATERIALS Vol. 14, No. 9- 10, September – October 2012, p. 758 - 762

# Photovoltaic effect of nanostructured $TiO_2$ layers in dye sensitized solar cells

SULE ERTEN-ELA
*Ege University, Solar Energy Institute, 35100, Bornova-Izmir, Turkey*

Metal-free organic sensitizer comprising donor, electron-conducting, and anchoring groups is engineered at a molecular level and synthesized for sensitization of mesoscopic titanium dioxide injection solar cells. The organic sensitizer anchored onto $TiO_2$ and is tested in dye sensitized solar cell with a volatile electrolyte system. In order to see the $TiO_2$ thickness dependence study of the triphenylene diamine based sensitizer on photovoltaic properties, we have fabricated dye sensitized solar cells having $TiO_2$ films of various thicknesses. The efficiency increased with the thickness of $TiO_2$ nanocrystalline layer; on the other hand, the photovoltage remained the same with increasing thickness. The increased surface area due to higher thickness of $TiO_2$ film allows for better light harvesting, which however enhances the possibility for injected electrons to recombine with the oxidized redox species triiodide. TPD-sensitized solar cell devices using a 10 (transparent) + 4 (scattering) $\mu$m thin $TiO_2$ layer yielded a short-circuit photocurrent density of 7.70 mA/cm$^2$, an open-circuit voltage of 800 mV, and a fill factor of 0.54, corresponding to an overall conversion efficiency of 3.34 % under standard AM 1.5 sun light.

(Received June 7, 2012; accepted September 20, 2012)

*Keywords*: Dye sensitized solar cells, Photovoltaics, Renewable energy, Nanoporous $TiO_2$

## 1. Introduction

Hybrid solar cells are typically composed of an electron transporting inorganic semiconductor material and a sensitizer material [1, 2]. A sensitizer, as the light-harvesting component in a dye-sensitized solar cell (DSSC), is of paramount importance to photovoltaic performance.

The sensitizer is attached to the surface of a mesoporous wide band-gap semiconductor serving as electron transporter [3, 4]. The critical factors that influence sensitization are the excited-state redox potential, which should match the energy of the conduction band edge of the oxide, light excitation associated with vectorial electron flow from the light-harvesting moiety of the dye toward the surface of the semiconductor surface, conjugation across the donor and anchoring groups, and electronic coupling between the lowest unoccupied molecular orbital (LUMO) of the dye and the $TiO_2$ conduction band. The major factors for low conversion efficiency of many organic dyes in the DSSC are the formation of dye aggregates on the semiconductor surface and recombination of conduction-band electrons with triiodide [5]. To overcome this drawback, researchers designed and developed novel dyes that not only provides an efficient electron transfer from the excited dye to the $TiO_2$ conduction band via good electronic coupling between the lowest unoccupied molecular orbital (LUMO) of the dye and the Ti 3d orbital but also minimizes aggregation. Therefore, to obtain optimal performance, aggregation of organic dyes and recombination need to be avoided through appropriate structural modification [6-8]. The interest in metal free, organic dyes with high extinction coefficients has grown in recent years for organic solar cell research.. In order to investigate organic dyes and, in the longer run, prepare an efficient solar cell dye, a number of different organic dyes are designed and synthesized [9-12].

In this paper, we report the effect of $TiO_2$ thickness dependence study using metal-free TPD organic sensitized solar cells. The TPD sensitizer have been used to manufacture solar cell devices to explore current-voltage characteristics by using 10 (transparent) + 4 (scattering) $\mu$m $TiO_2$ layers, 7 (transparent) + 5 (scattering) $\mu$m $TiO_2$ layers, 2 (transparent) + 4 (scattering) $\mu$m $TiO_2$ layers, respectively. TPD sensitizer exhibits a remarkable efficiency of 3.34 % using nanocrystalline 10 (transparent) + 4 (scattering) $\mu$m $TiO_2$ layers.

## 2. Experimental

### 2.1 Materials

Tetraphenylbenzidine, triphenyl phosphine, $POCl_3$, cyanoacetic acid and piperidine are purchased from Aldrich. Solvents are of spectroscopic grade and are used without any further purification.

### 2.2. Synthesis and characterization of triphenylene diamines consisting of anchoring groups

The synthesis of TPD dye is conducted in two steps with moderate yields. First reaction is Vilsmeier reaction, to form aldehyde product. In the second reaction, the aldehyde is condensed with cyanoacetic acid by means of the Knoevenagel reaction in the presence of piperidine to form the target compound of TPD (Fig. 1). Synthetic route of TPD is given in Fig. 2.

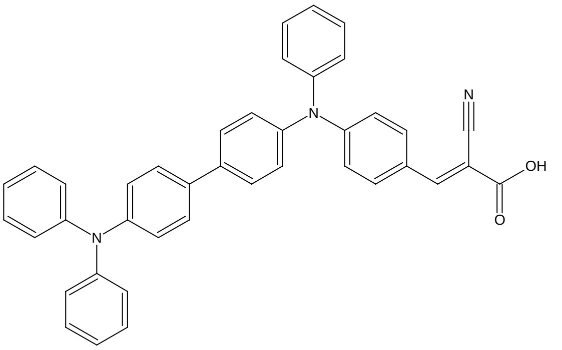

(*Z*)-2-cyano-3-4-[4-(4-diphenylaminophenyl)(phenyl)anilino]phenyl-2-propenoic acid, *TPD*

***Fig. 1.*** *Molecular structure of TPD dye*

### 2.3. Synthesis and characterization of TPD dye

**-Synthesis method of TPD**

Aldehyde product and acrylic acid product are synthesized in the following procedures.

**1. Step (synthesis of 4-[[4'-(diphenylamino)biphenyl-4-yl](phenyl)amino]benzaldehyde**

$POCl_3$ (1.36mmol, 0.2g) is stirred in a two-necked flask at 0 ºC for 1 hour in dried DMF under argon atmosphere. After additional stirring for 1 h at room temperature, this solution is added to a stirred solution of 5 g (0.0097 mol) of N,N’-Bis(diphenyl)benzidine in 20 mL of 1,2-dichloroethane. This reaction mixture is stirred for another hour at 60 °C and allowed to cool to room temperature. Hereafter the mixture is poured into a solution of 10 g sodium acetate in 100 mL water, and this mixture is extracted three times with dichloromethane. The combined organic layers are washed twice with water and dried over magnesium sulfate. After filtration and evaporation of the solvent a yellow solid is obtained. The desired monoformylated product is isolated from this crude product by column chromatography using silica gel and solvent as the eluent,

4-[[4'-(diphenylamino)biphenyl-4-yl](phenyl)amino]benzaldehyde, yellow crystals, Molecular structure is analysed with $^1H$ NMR spectrum. $^1H$ NMR ($CDCl_3$): (ppm), 9.83 (1H, s, -CHO), 7.71 (2H, d, Ar-H), 7.55 (2H, t, Ar-H), 7.48 (2H, t, Ar-H), 7.21 (21H, m, Ar-H).

**2. Step (Synthesis of (2*Z*)-2-(cyanomethyl)-3-{4-[[4'-(diphenylamino)biphenyl-4-yl](phenyl)amino]phenyl}acrylic acid, TPD)**

To a solution of 4-[[4'-(diphenylamino)biphenyl-4-yl](phenyl)amino]benzaldehyde (0.16mmol, 72.3mg) and cyanoacetic acid (0.32mmol, 27.95mg) in a mixture of tetrahydrofuran:methanol (1:1) is added catalytic amount of piperidine, after which the solution is stirred for 2 h at 40 °C. The solvent mixture is evaporated under reduced pressure and the resulting material is extracted with chloroform and 0.1M HCl solution, washed with water, and dried over magnesium sulfate. The product is purified by column chromatography using silicagel and chloroform:methanol as the eluent. Molecular structure is characterized with IR and $^1H$ NMR spectrum, Mass and Elemantal analysis. IR (KBr): $cm^{-1}$, 3551, 3412, 3031, 2214, 1583, 1487, 1392, 1323, 1270, 1178, 1074, 1028, 1003, 959, 818, 788, 749, 723, 693, 667. $^1H$ NMR (DMSO-$d_6$): (ppm), 7.88 (1H, s, -CH=), 7.79 (2H, d, Ar-H), 7.60 (4H, q, Ar-H), 7.36 (6H, m, Ar-H), 7.15 (5H, m, Ar-H), 7.10 (10H, m, Ar-H). MS/(ESI/100 eV): m/z: 583. $C_{40}H_{29}N_3O_2$ (583): Calcd: C 82.31%, H 5.01%, N 7.20%, O 5.48%; found: C 82.33%, H 5.00%, N 7.23%, O 5.48%.

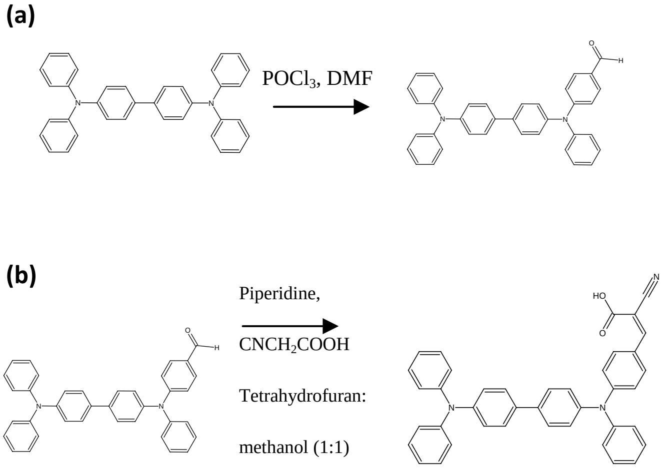

*Fig. 2. Synthetic route of TPD dyes consisting of anchoring groups, Vilsmeier reaction (a), Knovenagel reaction (b).*

## 3. Results and discussion

### 3.1. Electrochemistry of triphenylene diamine consisting of anchoring groups

$E_{HOMO}$ and $E_{LUMO}$ values of triphenylenediamine comprising anchoring groups are calculated by using cyclic voltammograms. Solutions of TPD dye are prepared in dichloromethane ($10^{-3}$ M). A three electrode cell set-up employed for the measurements consisted of glassy carbon working electrode, Pt wire counter electrode and Ag/AgCl reference electrode, all placed in a glass vessel. Tetrabutylamonium hexafluorophosphate ($TBAPF_6$), 0,1 M, is used as supporting electrolyte. Ferrocene is used as internal reference electrode. Fig. 3 and Table 1 summarize the voltammetric behavior of $10^{-3}$ M solution of TPD. TPD derivative shows both reduction and oxidation potential in Fig. 3. $E_{HOMO}$ and $E_{LUMO}$ levels are calculated from the onset potentials of oxidation and reduction and by assuming the energy level of ferrocene/ferrocenium ($Fc/Fc^+$) to be 4.8 eV below the vacuum level.

The oxidation of TPD, respectively proceeds by two successive one-electron oxidations. The oxidation products for TPD are stable on the voltammetric time scale, with halflives of at least several minutes in the solvents. Reduction process is observable for TPD molecules because of cyanoacetic acid side chain within the solvent window. TPD has low band gap (Table 1). According to $E_{LUMO}$ data of TPD, electrons can be injected into the conduction band of $TiO_2$ easily.

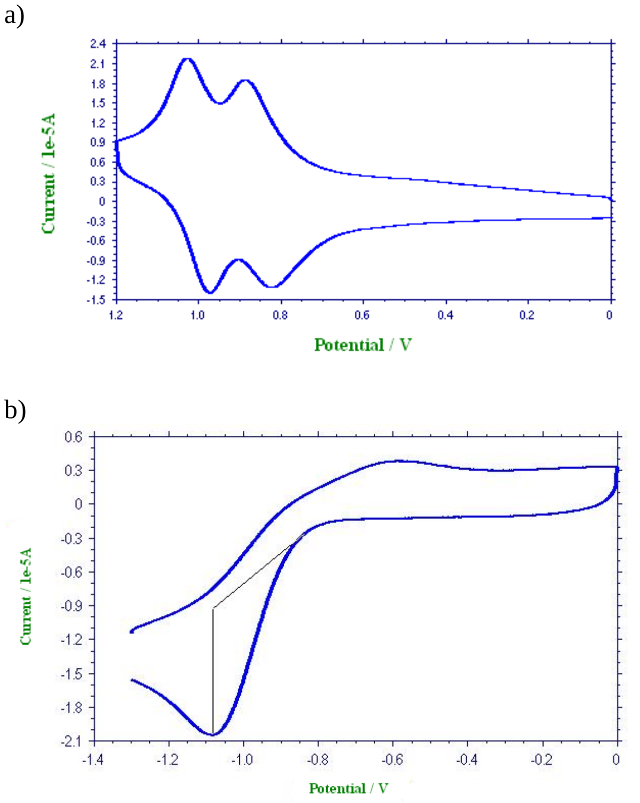

*Fig. 3. Cyclic voltammogram of TPD in positive (a) and negative region (b)*

*Table 1. Redox potentials of TPD derivatives.*

| | $E_{ox}$ [a] (Volt) | $E_{red}$ [b] (Volt) | $E_{ferrocene}$ [c] | $E_{HOMO}$ [d] | $E_{LUMO}$ [e] | $E_{BG}$ [f] |
|---|---|---|---|---|---|---|
| [TPD] | 0.85 | -1.08 | 0.39 | 5.26 | 3.33 | 1.93 |

[a] First oxidation potentials of TPD
[b] Reduction potentials of TPD
[c] Potentials of ferrocene, internal reference electrode
[d] HOMO energy level of TPD
[e] LUMO energy level of TPD
[f] Energy Band Gap of TPD

### 3.2. Photovoltaic device fabrication and characterization of DSSCs

FTO ($SnO_2$:F, Pilkington TEC-15; Rsheet:15O/&), electrically conductive oxide-coated glasses are used as transparent electrodes. The construction of the dye sensitized solar cell device requires first cleaning of the fluorine doped tin oxide (FTO) coated glass substrates in a detergent solution using an ultrasonic bath for 15 min, rinsed with water and ethanol. Both sensitizers have been used to manufacture solar cell devices to explore current-voltage characteristics using 10(transparent) + 4(scattering)μm $TiO_2$ transparent layers, 7(transparent) + 5(scattering) μm $TiO_2$ transparent layers, 2(transparent) + 4(scattering) μm $TiO_2$ transparent layers. Preparation and characterization of double-layer $TiO_2$ electrode are previously described by Wang [13] et al.

$TiO_2$-coated electrodes, after sintering at 450 $^0$C for 30 min and cooling to 100 $^0$C, and then $TiO_2$ electrodes are immersed into the TPD solution (0.5 mM in a mixture of acetonitrile: tert-butanol; chlorobenzene (volume ratio: 1:1:3) containing and kept at room temperature overnight. TPD adsorbed $TiO_2$-coated glasses are washed with pure chlorobenzene.

The stained electrode and Pt-counter electrode are assembled into a sealed sandwich-type cell by heating with a hot-melt ionomer film (Surlyn 1702, Du-Pont) as a spacer between the electrodes. Platinized FTO glasses are used as counter electrode. Platinization of counter electrodes is done by coating of FTO glasses with 1% solution of hydrogen hexachloroplatinate (Aldrich) in 2-propanol and annealing at 400 $^0$C for 30 min. Cells are prepared in sandwich geometry. Surlyn-1702 (DuPont) frame is used as a spacer and a thermoplastic sealant between the two electrodes. Cells prepared in this way are then sealed by heating at 100 $^0$C. A drop of electrolyte solution (electrolyte of 0.6M N-methyl-N-butyl-imidazolium iodide (BMII) + 0.1 M LiI + 0.05 M $I_2$ + 0.5 M 4-*tert*-butylpyridine (TBP) in acetonitrile) is placed on the drilled hole in the counter electrode of the assembled cell and is driven into the cell via vacuum backfilling. Finally, the hole is sealed using additional Bynel and a cover glass (0.1 mm thickness). Active areas of the cells are adjusted to 0.27 $cm^2$. Fig. 4 and Fig. 5 show the schematic drawing of dye sensitized solar cell.

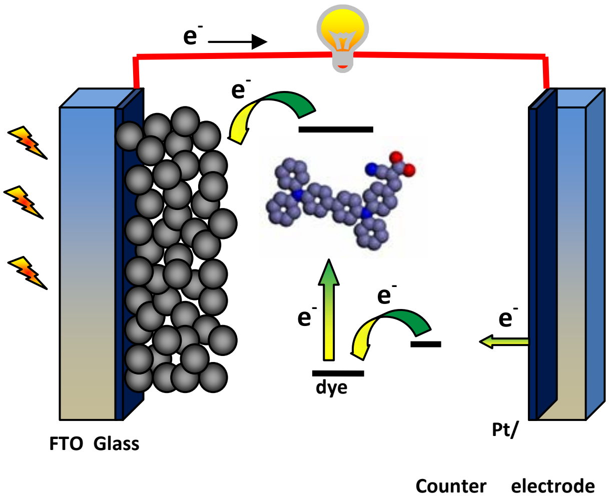

*Fig. 4. Schematic drawing of Dye Sensitized Solar Cell*

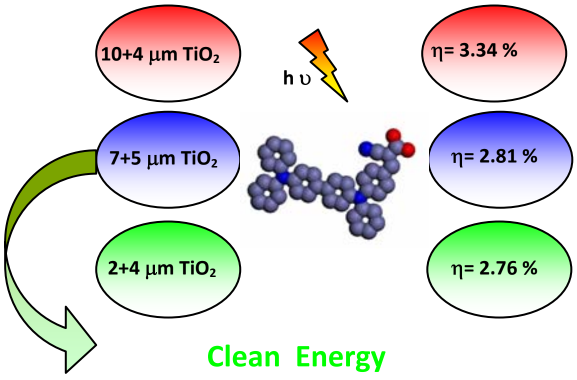

*Fig. 5. Schematic drawing for $TiO_2$ layers and efficiency*

$I - V$ data collection is made by using Keithley 2400 Source-Meter and LabView data acquisition software. $I - V$ characteristics of dye sensitized solar cell in dark and under illumination is shown in Fig. 6 .

### 3.3. Performances of Dye Sensitized Solar Cells

The TPD sensitizer has been used to manufacture solar cell devices to explore current-voltage characteristics by using 10 (transparent) + 4 (scattering) $\mu$m $TiO_2$, 7 (transparent) + 5 (scattering) $\mu$m $TiO_2$, 2 (transparent) + 4 (scattering) $\mu$m $TiO_2$ layers. Fig. 6 and Table 2 show the photovoltaic characterization of solar cells based on the TPD sensitizer using $TiO_2$ layers obtained with a sandwich cell using electrolyte of 0.6M N-methyl-N-butyl-imidazolium iodide (BMII) + 0.1 M LiI + 0.05 M $I_2$ + 0.5 M 4-*tert*-butylpyridine (TBP) in acetonitrile as redox electrolyte. In order to see the effect of thickness layers of $TiO_2$ on photovoltaic properties, we have fabricated dye sensitized solar cells having $TiO_2$ films of various thicknesses and using TPD sensitizer. The photocurrent increased with the thickness of $TiO_2$ nanocrystalline layer; on the other hand, the photovoltage remained the same with increasing thickness (see Table 2). The increased surface area due to higher thickness of $TiO_2$ film allows for better light harvesting, which however enhances the possibility for injected electrons to recombine with the oxidized redox species triiodide. Under standard global AM 1.5 solar conditions, the TPD-sensitized cell devices using a 10 (transparent) + 4 (scattering) $\mu$m thin $TiO_2$ layer gave a short-circuit photocurrent density ($J$sc) of 7.70 mA/cm$^2$, an open-circuit voltage ($V$oc) of 800, and a fill factor ($ff$) of 0.54, corresponding to an overall conversion efficiency $\eta$,derived from the equation $\eta$ ) $J$sc $V$oc $ff$ /light intensity, of 3.34 % (see Table 2). The device using a 7 (transparent) + 5 (scattering) $\mu$m thin $TiO_2$ layer gave $J$sc of 7.71 mA/cm$^2$, $V$oc of 800 mV, and $ff$ of 0.45, corresponding to an overall conversion efficiency $\eta$ of 2.81%. Current-voltage characteristics of TPD using 2 (transparent) + 4 (scattering) $\mu$m $TiO_2$ performed 800 mV open circuit voltage, 5.82 mA/cm$^2$ short-circuit current, 0.59 fill factor and 2.76 % overall conversion efficiency.

In line with these statements, we now report the good efficiency under standard conditions obtained for TPD sensitizer using 10 (transparent) + 4 (scattering) $\mu$m $TiO_2$ layers that shows 800 mV open circuit voltage, 7.70 mA/cm$^2$ short-circuit current, 0.54 fill factor and 3.34 % overall conversion efficiency.

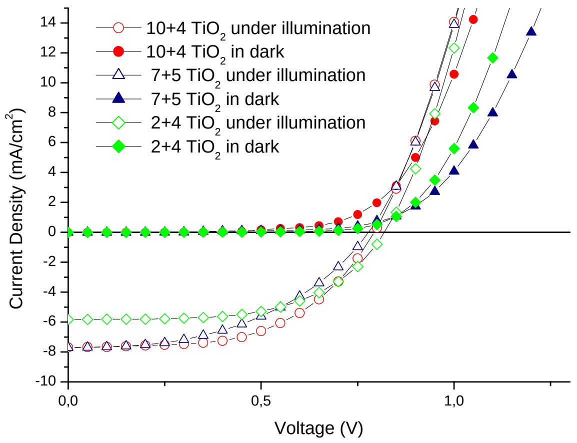

*Fig. 6. I-V characteristics of dye sensitized solar cell with TPD dye using electrolyte consisting of 0.6M N-methyl-N-butyl-imidazolium iodide (BMII) + 0.1 M LiI + 0.05 M $I_2$ + 0.5M TBP under simulated AM 1.5 (100 mWcm$^{-2}$) illumination.*

*Table 2. Photovoltaic characterization of TPD dye using different $TiO_2$ thickness layers*

| Thickness (µm) | $J_{sc}$ (mAcm$^{-2}$) | $V_{oc}$ (mV) | FF | η (%) |
|---|---|---|---|---|
| 10 + 4 | 7.70 | 800 | 0.54 | 3.34 |
| 7 + 5 | 7.71 | 800 | 0.45 | 2.81 |
| 2 + 4 | 5.82 | 800 | 0.59 | 2.76 |

## 4. Conclusion

In this paper, we have successfully fabricated dye sensitized solar cells using metal-free organic dye (TPD) that contain novel donor-bridge-acceptor molecules. We investigated the effect of different $TiO_2$ thickness layers on photovoltaic properties. We report the good efficiency obtained with 10 (transparent) + 4 (scattering) μm $TiO_2$ transparent layers under standard conditions for TPD dye that performs 800 mV open circuit voltage, 7.70 $mA/cm^2$ short-circuit current, 0.54 filling factor and 3.34 % overall conversion efficiency.

**Acknowledgement**

I thank the Alexander von Humboldt Foundation (AvH) for supporting me scientifically. Also I thank Scientific Research Council of Turkey (TUBITAK). I thank Mechanical Engineer MSc. Cagatay ELA for his unending support and fruithful advices.

## References

[1] B. O'Regan, M. Graetzel, Nature **353**, 737 (1991)
[2] D. Rana Bekci, S. Erten-Ela, Renewable Energy **43**, 378 (2012).
[3] a) S. Erten-Ela, S. Cogal, G. Turkmen, S. Icli, Curr Appl Phys **10**, 187 (2010).
b) A. C. Cakir, P. Guloglu, M. Bilgin, S. Erten-Ela, Journal of Optoelectronics and Advanced Materials, **14**, 230 (2012).
[4] H. Qin, S. Wenger, M. Xu, F. Gao, X. Jing, P. Wang, S. M. Zakeeruddin, M. Graetzel, J. Am. Chem. Soc. **130,** 9202 (2008).
[5] a) S. Kolemen, A. Bozdemir, Y. Cakmak, G. Barin, S. Erten-Ela, M. Marszalek, J-H. Yum, S.M Zakeeruddin, M.K. Nazeeruddin, M. Graetzel, Akkaya E.U Chemical Science, **2**, 949 (2011).
b) S. Erten-Ela., M. D. Yilmaz, B. Icli, Y. Dede, S. Icli, and E. U. Akkaya, Organic Letters **10**, 3299 (2008).
c) S. Kolemen, Y. Cakmak, S. Erten-Ela, Y. Altay, J. Brendel, M. Thelakkat and EU. Akkaya, Organic Letters **12**, 3812, (2010).
[6] P.Y. Reddy, L. Giribabu, C. Lyness, H.J. Snaith et al Angew. Chem. Int. Ed. **46**, 373(2007)
[7] J.J Cid, J.H. Yum, S.R. Jang, M.K Nazeeruddin et al Angew. Chem. Int. Ed**. 46,** 8358(2007)
[8] D.P. Hagberg, J.H. Yum, H. Lee et al J. Am. Chem. Soc. **130**,6259 (2008)
[9] S. Erten-Ela, S. Cogal, S. Icli, Optoelectron. Adv. Mater. - Rapid Commun. **3**, 459 (2009).
[10] a) S. Erten-Ela, S. Cogal, S. Icli, Inorg. Chim. Acta **362**, 1855 (2009)
b) S. Erten-Ela, J. Brendel, M. Thelakkat, Chemical Physics Letters, **510**, 93 (2011).
[11] a)S. Erten-Ela, M. Marszalek et al Curr. App. Phys **10**,749 (2010),
b) A. Cagatay Cakir, Sule Erten-Ela, Advanced Powder Technology, **23**, 655 (2012).
[12] S. Wenger, P-A. Bouit, Q. Chen, J. Teuscher, D. Censo, R. Humphry-Baker, J-E. Moser, J.L. Delgado, N. Martin, S.M. Zakeeruddin, M. Graetzel J. Am. Chem. Soc. **132**, 5164 (2010).
[13] (a) C. Li, W. Wang, X. Wang,et al Chem. Lett., **34**, 554 (2005) (b) A. Burke, L.S. Mende, S. Ito, M. Grätzel Chem Commun **3**, 234 (2007).

---

[*] Corresponding author: suleerten@yahoo.com, sule.erten@ege.edu.tr